Shell-Model Calculations for ^{22}Na and ^{22}Ne

B. M. Preedom

Department of Physics, University of South Carolina, Columbia, South Carolina 29208,
and Cyclotron Laboratory,* Michigan State University, E. Lansing, Michigan 48823

and

B. H. Wildenthal*

Cyclotron Laboratory,* and Department of Physics, Michigan State University, E. Lansing, Michigan 48823

Shell-model calculations have been performed for the nuclei ^{22}Na and ^{22}Ne. The model space is made up of all Pauli-allowed combinations of six particles in the orbits $0d_{5/2}$, $1s_{1/2}$, and $0d_{3/2}$. An inert ^{16}O core is assumed. The two-body interaction which is employed has been obtained by empirically modifying some of the matrix elements of Kuo's interaction in order to achieve an rms best fit between the observed energies of 72 levels in the $A = 18$–22 region and the corresponding shell-model eigenvalues. Single-particle energies are taken from the ^{17}O spectrum. Calculated results for excitation energies, electromagnetic transition strengths, and spectroscopic factors for single-nucleon transfer are presented and compared with existing data.

I. INTRODUCTION

The shell model has been used successfully to describe the low-lying spectra of nuclei near neutron and proton closed shells. With the advent of sophisticated computer codes,[1] it has become possible to calculate the properties of nuclei further from closed shells. In particular, it has been shown that many aspects of the collective features of nuclei several nucleons removed from ^{16}O in the s-d shell can be well reproduced by shell-model calculations in which all of the s-d nucleons are active.[2–5]

Several aspects of the $A = 22$ nuclei make them of particular interest from the standpoint of attempting to understand collective nuclear phenomena in terms of many-body microscopic calculations. These systems appear to be among the most highly deformed nuclei in the light-mass region. In addition, there have been extensive experimental studies of ^{22}Na and ^{22}Ne which have assigned spins and parities to many low-lying levels and have measured the strengths of many electric quadrupole and single-nucleon transfer transitions.

Since one wants to observe the fullest consequences of the two-body part of the nuclear Hamiltonian, it is desirable to study systems with as many active particles as possible. If the active particles are distributed without restriction over the three sd-shell orbits, the shell-model states for $A = 22$ have dimensions as large as can be handled straightforwardly with our techniques. The $A = 22$ systems thus constitute the best place to study the many-particle shell-model structure in

this region if one is to avoid introducing the additional complication of basis truncation within the s-d shell space itself.

Finally, the $A = 22$ systems are of interest because, despite significant successes in explaining some features of their behavior, several aspects of the structure of the low-lying levels seemed to be reproduced poorly by previous calculations.[2, 3, 5] In general, the results of shell-model calculations reproduce the detailed features of doubly odd nuclei less successfully than those of doubly even and even-odd nuclei. Thus a fully successful accounting for the properties of ^{22}Na would significantly increase confidence in the shell-model description of the structure of nuclei in this region.

II. TECHNIQUES OF CALCULATION

The shell-model calculations presented here are of the same type as those presented in Ref. 2, hereafter referred to as HMWP, and the notations and conventions of this reference are used in the present paper. The derivation of the Hamiltonian used in the present work is discussed in detail in Ref. 6. Briefly, the single-particle energies were taken from the observed spectrum of ^{17}O. For the $0d_{5/2}$, $1s_{1/2}$, and $0d_{3/2}$ orbits they are equal to -4.15, -3.28, and $+0.93$ MeV, respectively. The two-body matrix elements were obtained by adjusting selected two-body matrix elements of the "$K + ^{17}$O" interaction used in HMWP so as to reach an rms best fit between 72 experimental-level energies in the $A = 18$–22 region and the corresponding shell-model eigenvalues.

The "$K + ^{17}$O" interaction of HMWP is one of the

realistic effective interactions calculated from the Hamada-Johnston potential by Kuo.[7] Those two-body matrix elements of "$K + {}^{17}O$" which do *not* involve the $d_{3/2}$ orbit were varied as free parameters in the fit procedure. In addition, the centroids of the $d_{5/2}$-$d_{3/2}$ and $d_{3/2}$-$d_{3/2}$ interactions were varied. All of the low-lying $T = 0$ levels in mass 22 were included in the fitting-data set, in addition to the two 0^+, $T = 1$ levels.

The eigenvalues and eigenvectors which are obtained for $A = 18$–21 nuclei with this new interaction[6] are similar in most aspects to those obtained[2] with "$K + {}^{17}O$," but quantitative agreement with experiment is somewhat better in essentially all cases. The main qualitative changes in the $A = 18$–21 region which result from use of the new interaction are a raising of the centroids of the $s_{1/2}$ and $d_{3/2}$ single-particle strengths and a lessening of the level densities in the low-excitation-energy part of the spectra. The two-body matrix elements of both the original "$K + {}^{17}O$" and of the

modified interaction used in the present work are listed in Table I.

The excitation energies and wave functions for states in the $A = 22$ nuclei were taken as the eigenvalues and eigenvectors of the Hamiltonian matrix for a given J, T. The largest matrix in the present study was 537×537 for the 3^+, $T = 1$ states. The evaluation of the Hamiltonian matrix elements was done with the Oak-Ridge-Rochester shell-model codes.[1]

Spectroscopic factors for single-nucleon-transfer transitions to states of a given nucleus are a primary key to the identification of a calculated state with an experimental level. The spectroscopic factors, S, presented here are calculated as in HMWP. In an isospin formalism S is independent of T_z, whereas the calculated cross section for the transfer to a particular nucleus is proportional to $C^2 S$, where C is a Clebsch-Gordan coefficient dependent on T_z. The spectroscopic factor for a $0d_{5/2}$ particle transfer from a state

TABLE I. The two-body matrix elements $\langle j_a j_b J T | V | j_c j_d J T \rangle$. The units are MeV and the phase conventions are from HMWP.

$2j_a$	$2j_b$	$2j_c$	$2j_d$	$,JT$	Present	Kuo[a]	$2j_a$	$2j_b$	$2j_c$	$2j_d$	$,JT$	Present	Kuo[a]
5	5	5	5	,01	−2.1243	−2.4381	5	3	5	3	,10	−5.3692	−5.8276
5	5	5	5	,10	−0.9437	−1.0284	5	3	5	3	,11	0.4058	−0.1257
5	5	5	5	,21	−1.2312	−1.0358	5	3	5	3	,20	−4.0520	−4.5271
5	5	5	5	,30	−1.7788	−0.8589	5	3	5	3	,21	0.3268	−0.2037
5	5	5	5	,41	0.1611	−0.0502	5	3	5	3	,30	−0.6127	−1.1313
5	5	5	5	,50	−4.0232	−3.6640	5	3	5	3	,31	0.6664	0.1316
5	5	5	1	,21	−0.6594	−0.8542	5	3	5	3	,40	−3.8359	−4.3137
5	5	5	1	,30	−1.1865	−1.5654	5	3	5	3	,41	−1.1485	−1.6603
5	5	5	3	,10	3.2056	3.1651	5	3	1	1	,10	1.7345	1.7125
5	5	5	3	,21	−0.4020	−0.3969	5	3	1	3	,10	−1.9378	−1.9132
5	5	5	3	,30	1.8986	1.8746	5	3	1	3	,11	−0.0989	−0.0976
5	5	5	3	,41	−1.3801	−1.3626	5	3	1	3	,20	−1.5602	−1.5404
5	5	1	1	,01	−1.4058	−0.9677	5	3	1	3	,21	−0.7796	−0.7697
5	5	1	1	,10	−0.4241	−0.5959	5	3	3	3	,10	0.0388	0.0383
5	5	1	3	,10	−0.2399	−0.2368	5	3	3	3	,21	−1.0230	−1.0101
5	5	1	3	,21	−0.8471	−0.8364	5	3	3	3	,30	2.1856	2.1579
5	5	3	3	,01	−3.8367	−3.7882	1	1	1	1	,01	−2.2643	−1.9493
5	5	3	3	,10	1.6417	1.6209	1	1	1	1	,10	−3.4227	−3.1839
5	5	3	3	,21	−0.9149	−0.9034	1	1	1	3	,10	0.3125	0.3085
5	5	3	3	,30	0.5060	0.4996	1	1	3	3	,01	−0.7543	−0.7448
5	1	5	1	,20	0.1766	−0.6222	1	1	3	3	,10	−0.2154	−0.2127
5	1	5	1	,21	−0.8495	−1.2879	1	3	1	3	,10	−2.7861	−3.2771
5	1	5	1	,30	−3.6603	−3.6919	1	3	1	3	,11	0.7525	0.2167
5	1	5	1	,31	0.7838	0.1723	1	3	1	3	,20	−1.0974	−1.6099
5	1	5	3	,20	−1.4674	−1.4488	1	3	1	3	,21	0.2022	−0.3267
5	1	5	3	,21	−0.2209	−0.2181	1	3	3	3	,10	0.8097	0.7995
5	1	5	3	,30	1.1709	1.1561	1	3	3	3	,21	−0.2097	−0.2071
5	1	5	3	,31	−0.0903	−0.0892	3	3	3	3	,01	−0.2849	−0.8076
5	1	1	3	,20	−2.6118	−2.5788	3	3	3	3	,10	0.0576	−0.4695
5	1	1	3	,21	−1.5710	−1.5511	3	3	3	3	,21	0.6110	0.0770
5	1	3	3	,21	−0.7531	−0.7436	3	3	3	3	,30	−2.0873	−2.5872
5	1	3	3	,30	0.0272	0.0269							

[a] Reference 7.

Ψ^{JT} having n active nucleons to a state $\psi^{J_0 T_0}$ having $n-1$ active nucleons is

$$S(0d_{5/2}) = n \langle \Psi^{JT}_{J_z T_z}(1 \ldots n) | [\psi^{J_0 T_0}(1 \ldots n-1) \phi_{0d}^{j=5/2,\,t=1/2}(n)]^{JT}_{J_z T_z} \rangle^2 \, ,$$

where $\phi_{0d}^{j=5/2,\,t=1/2}(n)$ is the $0d_{5/2}$ single-particle wave function for the nth nucleon. Analogous definitions hold for $0d_{3/2}$ and $1s_{1/2}$ nucleon transfer. Spectroscopic factors will hereafter be written as $S(d_{5/2})$, $S(d_{3/2})$, and $S(s_{1/2})$. When both $j = \frac{3}{2}$ and $j = \frac{5}{2}$ transfers are allowed to the same states, the factor

$$S(l=2) = S(d_{3/2}) + S(d_{5/2})$$

TABLE II. Excitation energies in MeV for $A = 22$, $T = 0$. Excitation energy is taken as the energy increment above the 3^+_1 state. The shell-model energy for this state is calculated to be -58.45 MeV compared with the experimental value of -58.52 MeV (with Coulomb contributions removed).

J_n	Exp[a]	Present	HMWP
0_1		7.54	5.41
0_2		10.14	8.25
1_1	0.58	0.22	−0.31
1_2	1.94	1.85	0.24
1_3	3.94	3.79	2.60
1_4	4.32	5.48	4.48
2_1	3.06	2.60	0.77
2_2	(4.36)	3.23	1.99
2_3		4.93	3.17
2_4		5.33	4.06
3_1	0	0	0
3_2	1.98	1.59	0.93
3_3	2.97	2.88	1.86
3_4		4.16	2.96
4_1	0.89	0.86	0.81
4_2		4.34	2.59
4_3		5.00	4.13
4_4		5.80	5.28
5_1	1.53	1.47	
5_2	(4.71)	4.44	
5_3		5.24	
6_1	(3.71)	3.83	
6_2		6.79	
6_3		7.48	
7_1		4.56	
7_2		8.47	
8_1		8.15	
8_2		11.51	
9_1		10.03	
9_2		13.09	
10_1		13.41	

[a]Where a spin assignment is tentative, the excitation energy is in parentheses.

will be compared with the experimental value.

Electromagnetic transition rates and moments are also calculated as in HMWP. The electric quadrupole operator is taken as

$$\underline{Q}^2 = (\bar{e}_p + \bar{e}_n) \sum_{k=1}^{A} \tfrac{1}{2} r_k^2 \underline{Y}^2(\Omega_k) + (\bar{e}_p - \bar{e}_n) \sum_{k=1}^{A} t_z(k) r_k^2 \underline{Y}^2(\Omega_k),$$

where $\bar{e}_p = 1.5e$ and $\bar{e}_n = 0.5e$ are assumed as the

TABLE III. Excitation energies in MeV for $A = 22$, $T = 1$. Excitation energy is taken as the energy increment above the 0^+_1 state. The shell-model energy for this state is calculated to be -57.79 MeV compared with the experimental value of -57.75 MeV (with Coulomb contributions removed).

J_n	Exp (^{22}Ne)[a]	Exp (^{22}Na)	Present	HMWP
0_1	0	0	0	0
0_2	(6.24)	6.18	5.98	4.95
0_3			7.02	6.81
1_1	(5.36)		5.03	5.18
1_2			6.48	5.45
1_3			8.25	
1_4			8.82	
2_1	1.28	1.29	1.39	1.14
2_2	4.46	4.51	4.14	3.53
2_3	(5.33)		4.80	4.77
2_4			6.05	5.43
3_1	(5.64)		5.41	4.51
3_2			6.30	
3_3			7.40	
3_4			8.14	
4_1	3.36	3.41	3.49	3.21
4_2	5.52		5.49	5.54
4_3			6.43	
4_4			6.84	
5_1			7.49	
5_2			8.61	
6_1	6.35		6.41	6.30
6_2			9.24	
7_1			10.88	
7_2			11.90	
8_1	11.01		11.13	
8_2			12.62	
9_1			15.50	
10_1			16.34	

[a]Where a spin assignment is tentative, the excitation energy is in parentheses.

total effective charges of the proton and neutron, respectively, r_k is the radial coordinate of the kth nucleon, and Y^2 is the usual spherical harmonic operator of rank 2. The convention $t_z = \frac{1}{2}$ for a proton and $t_z = -\frac{1}{2}$ for a neutron is chosen.

For the electric quadrupole moment Q of a many-particle state $\psi_{T_z}^{JT}(\alpha)$,

$$Q = (\tfrac{16}{5}\pi)^{1/2}\langle \alpha JT, J_z=J, T_z | Q_0^2 | \alpha JT, J_z=J, T_z \rangle,$$

where Q_0^2 is the z component of $\underline{Q}^2$.

For an $E2$ transition from $\psi_{T_{zi}}^{J_i T_i}(\alpha_i)$ to $\psi_{T_{zf}}^{J_f T_f}(\alpha_f)$ the reduced transition amplitude is taken as

$$B(E2)_{i \to f} = (2J_i + 1)^{-1}\langle \alpha_f J_f T_f, T_{z_f} \| \underline{Q}^2 \| \alpha_i J_i T_i, T_{z_i} \rangle^2,$$

where the reduced matrix element is reduced with respect to J only. In order to evaluate this matrix element, single-nucleon wave functions in each $\psi^{JT}(\alpha)$ were taken as harmonic-oscillator wave functions with $\hbar\omega = 14.6$ MeV.

TABLE IV. Transition rates for ^{22}Na $T=0 \to T=0$ transitions.

$J_n(i) \to J_m(f)$		$B(E2)$ $(e^2 \text{ F}^4)$	$B(M1)$ $(10^{-3}\,\mu_N^2)$	$J_n(i) \to J_m(f)$		$B(E2)$ $(e^2 \text{ F}^4)$	$B(M1)$ $(10^{-3}\,\mu_N^2)$
1_1	3_1	0.10		4_2	2_2	0.15	
1_2	1_1	0.16	18	4_2	3_1	1.6	0.20
1_2	3_1	12		4_2	3_2	0.10	8.2
1_2	3_2	0.87		4_2	3_3	22	6.0
1_3	1_1	0.05	0.18	4_2	4_1	1.5	0.01
1_3	1_2	0.01	3.8	4_2	5_1	2.9	0.8
1_3	2_1	4.7	0.20	4_2	6_1	4.5	
1_3	2_2	1.2	3.8	4_3	2_1	0.86	
1_3	3_1	0.21		4_3	2_2	30	
1_3	3_2	0.42		4_3	3_1	2.3	2.3
				4_3	3_2	4.9	0.0
2_1	1_1	0.03	10	4_3	4_1	2.1	1.1
2_1	1_2	95	3.9				
2_1	3_1	3.3	0.10	5_1	3_1	21	
2_1	3_2	0.89	7.1	5_1	4_1	79	1.4
2_1	4_1	4.0		5_2	3_1	0.32	
2_2	1_1	5.4	0.06	5_2	3_2	54	
2_2	1_2	0.02	4.2	5_2	3_3	14	
2_2	2_1	0.00	2.2	5_2	4_1	0.62	0.00
2_2	3_1	0.58	16	5_2	4_2	2.6	5.3
2_2	3_2	0.59	0.02	5_2	5_1	1.8	0.00
2_2	3_3	19	1.0	5_2	6_1	1.5	0.00
2_2	4_1	0.01					
2_3	1_1	0.82	0.33	5_3	3_1	1.5	
2_3	1_2	1.0	1.8	5_3	4_1	5.9	1.2
2_3	1_3	38	2.0				
2_3	2_1	1.4	0.00	6_1	4_1	32	
2_3	2_2	1.2	3.2	6_1	5_1	57	1.8
2_3	3_i	3.5	8.6	6_2	4_1	0.57	
2_3	3_2	0.01	0.00	6_2	4_2	42	
				6_2	4_3	5.8	
3_2	1_1	69		6_2	5_1	2.0	2.2
3_2	3_1	0.06	0.00				
3_2	4_1	0.18	0.09	7_1	5_1	38	
3_2	5_1	0.90		7_1	5_2	1.5	
3_3	1_1	0.19		7_1	6_1	45	2.4
3_3	1_2	34		7_2	5_1	0.35	
3_3	2_1	22	0.34	7_2	5_2	50	
3_3	3_1	0.00	0.04	7_2	6_1	0.02	0.26
3_3	3_2	0.63	10				
3_3	4_1	8.8	0.01	8_1	6_1	34	
3_3	5_1	9.7		8_2	6_1	1.9	
				8_1	6_2	17	
4_1	3_1	90	0.75	8_2	6_2	23	
4_2	2_1	66		8_1	7_1	30	5.3
				8_2	7_1	0.31	0.55
				9_1	7_1	24	
				9_2	7_1	0.08	

FIG. 1. Calculated excitation energies for the $K = 3$, $T = 0$; $K = 0$, $T = 0$; and $K = 0$, $T = 1$ band members displaying the rotational $J(J + 1)$ dependence.

TABLE V. Transition rates for ^{22}Na ($T_z = 0$) and ^{22}Ne ($T_z = -1$) $T = 1 \rightarrow T = 1$ transitions.

$J_n(i) \rightarrow J_m(f)$	$B(E2)$ $(e^2 F^4)$ ^{22}Ne	^{22}Na	$J_n(i) \rightarrow J_m(f)$	$B(E2)$ $(e^2 F^4)$ ^{22}Ne	^{22}Na
$2_1 \quad 0_1$	48	56	$5_2 \quad 4_2$	1.3	
$2_2 \quad 0_1$	3.7	2.4	$6_1 \quad 4_2$	0.11	
$0_2 \quad 2_1$	15	13	$6_2 \quad 4_2$	11	
$0_2 \quad 2_2$	9.0	3.7	$4_3 \quad 2_1$	0.06	
$3_1 \quad 1_1$	2.4		$4_3 \quad 2_2$	12	
$3_2 \quad 1_1$	19		$4_3 \quad 2_3$	5.2	
$1_1 \quad 2_1$	6.0		$5_1 \quad 3_1$	8.5	
$1_1 \quad 2_2$	35		$5_1 \quad 3_2$	2.2	
			$5_2 \quad 3_1$	28	
$2_2 \quad 2_1$	1.4	4.2	$5_2 \quad 3_2$	0.90	
$2_3 \quad 2_1$	5.2	6.8	$6_2 \quad 5_1$	39	
$2_4 \quad 2_1$	0.34	1.0	$6_2 \quad 5_2$	1.0	
$3_1 \quad 2_1$	2.2				
$3_2 \quad 2_1$	0.86		$7_1 \quad 5_1$	11	
$4_1 \quad 2_1$	66	71	$7_1 \quad 5_2$	4.9	
$4_2 \quad 2_1$	0.65	0.39	$7_1 \quad 6_1$	0.00	
$3_1 \quad 2_2$	47		$7_1 \quad 6_2$	20	19
$3_2 \quad 2_2$	1.0		$7_2 \quad 5_1$	4.3	
$4_2 \quad 2_2$	9.3		$7_2 \quad 5_2$	24	
			$7_2 \quad 6_1$	1.2	
$2_2 \quad 4_1$	0.05		$7_2 \quad 6_2$	3.4	
$3_1 \quad 4_1$	0.79		$7_2 \quad 8_1$	3.5	
$3_2 \quad 4_1$	1.5				
$4_2 \quad 4_1$	0.90		$8_1 \quad 6_1$	30	36
$5_1 \quad 4_1$	0.81		$8_1 \quad 6_2$	0.77	
$5_2 \quad 4_1$	0.41		$8_1 \quad 7_1$	1.2	
$6_1 \quad 4_1$	53	62	$8_2 \quad 6_1$	5.0	7.1
$6_2 \quad 4_1$	0.07	0.00	$8_2 \quad 6_2$	11	
			$8_2 \quad 7_1$	9.6	
$3_2 \quad 4_2$	0.68				
$5_1 \quad 4_2$	44				

For magnetic dipole transitions from $\psi_{T_{zi}}^{J_i T_i}(\alpha_i)$ to $\psi_{T_{zf}}^{J_f T_f}(\alpha_f)$, the reduced transition probability is taken as

$$B(M1)_{i \rightarrow f} = (2J_i + 1)^{-1} \langle \alpha_f J_f T_f, T_{z_f} \| \underline{M}^1 \| \alpha_i J_i T_i, T_{z_i} \rangle^2 ,$$

where again the reduced matrix element is reduced with respect to J only. The operator $\underline{M}^1$ is taken to be the unperturbed free-nucleon $M1$ operator

$$\underline{M}^1 = \sum_{k=1}^{A} \tfrac{1}{2} [\, \vec{l}(k) + (g_p + g_n) \vec{s}(k)]$$

$$+ \sum_{k=1}^{A} t_z(k) [\vec{l}(k) + (g_p - g_n) \vec{s}(k)] ,$$

where $\vec{l}(k)$ and $\vec{s}(k)$ are the orbital and spin angular momenta of nucleon k; the units are nuclear magnetons, μ_N, and the convention $t_z = +\tfrac{1}{2}$ for a proton and $t_z = -\tfrac{1}{2}$ for a neutron has again been chosen. The free-nucleon orbital and spin gyromagnetic ratios for the neutron and proton have been assumed.

The magnetic dipole moment μ of a many-particle shell-model state $\mu^{JT}(\alpha)$ is calculated from

$$\mu = \langle \alpha J T J_z = J T_z \, | M_0^1 | \, \alpha J T J_z = J T_z \rangle ,$$

where M_0^1 has only the z component of the vector operators $\vec{l}$ and $\vec{s}$ in $\underline{M}^1$.

III. RESULTS

A. Excitation Energies

Calculated and measured[8,9] energies for the $A = 22$, $T = 0$ levels are presented in Table II. The new results are in noticeably better agreement with experiment than are those of the HMWP calculation, in particular for the 1^+ states and the states outside of the ground-state 3^+, 4^+, 5^+ band. In their study comparing the results of seven dif-
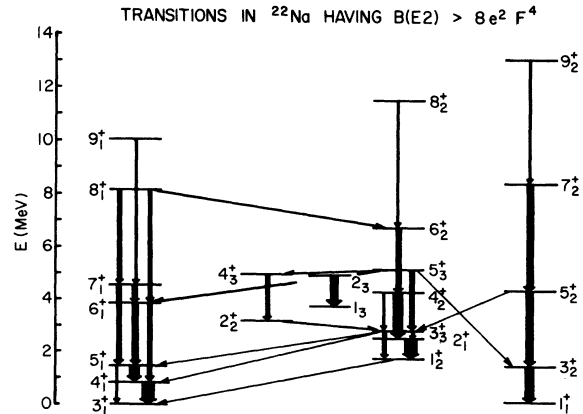
FIG. 2. Calculated transition rates for $T = 0 \rightarrow T = 0$ transitions in ^{22}Na.

TABLE VI. $B(E2, J_i \to J_f)$ for ^{22}Na $(e^2\,F^4)$ $T = 0 \to T = 0$.

J_i	J_f	Exp	Present	HMWP	Arima et al.[a]	Rotational[b]
4_1	3_1	94 ± 15 [c]	90	101.4	3.07	93.9
5_1	4_1	59 ± 8 [c]	79	90.9	40.02	87.8
5_1	3_1	20 ± 3 [c]	21	25.2	9.75	22.8
6_1	5_1		57	69.2		71.7
6_1	4_1		32	37.9		40.5
3_2	1_1		69	66.0	7.33	
5_2	3_2		54		0.186	
1_2	3_1		12		0.150	
1_1	3_1	0.03 ± 0.01 [d]	0.10	5.5	155.0	
3_2	3_1		0.06	0.2		
5_2	3_1		0.32			63.42
5_2	4_1		0.62			53.09

[a] Reference 5.
[b] Rotational model calculated by HMWP.
[c] Data of Ref. 14 as adjusted by HMWP.
[d] Reference 15.

ferent Hamiltonians, HMWP found that only two produced spectra in which the first 1^+ state came above the first 3^+ state. These two Hamiltonians however were not as successful as the "$K + {}^{17}$O" interaction in accounting for various other observables in the $A = 18$–22 mass region. In addition to improving the agreement with the $T = 0$ states, the relative spacings between the $T = 0$ and $T = 1$ states are also well reproduced. This $0^+(T = 1)$–$3^+(T = 0)$ spacing has been previously described by Kelson in terms of an even-even core rotator with two odd nucleons coupled to it.[10]

The calculated and observed[11] excitation energies for the $A = 22$, $T = 1$ levels are presehted in
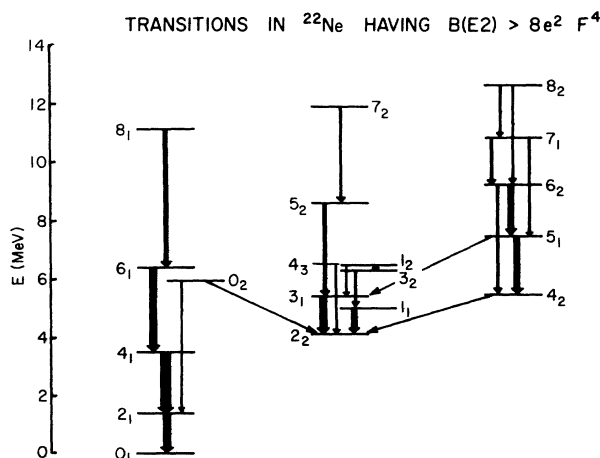
Table III. The assignment of 0^+ to the 6.24-MeV state is by Scholz et al.,[12] and that of 8^+ to the 11.01-MeV state by Broude et al.[13] The present calculation again represents an improvement over previous calculations in agreement with observation. Comparing the present calculation with that of HMWP, it is seen that the 2^+ (4.14-MeV), 3^+ (5.41-MeV), 0^+ (5.98-MeV), and the 1^+ (6.48-MeV) states are all in better energy agreement with their possible experimental counterparts. A comparison with the calculation of Akiyama et al.[3] shows that the locations of the 2^+ (4.14-MeV), 1^+ (5.03-MeV), 3^+ (5.41-MeV), and 2^+ (6.41-MeV) states are in better agreement with experiment.

The observed levels of these nuclei are often interpreted in terms of rotations of intrinsically deformed shapes. The energies of levels in a rotational "band" ideally increase linearly with the quantity $J(J+1)$. The energies we calculate in the shell model exhibit this sort of behavior up to quite high J values. In Fig. 1, the calculated energies are grouped into what might be called $K = 3$, $T = 0$; $K = 0$, $T = 0$; and $K = 0$, $T = 1$ bands and plotted against $J(J+1)$. There is striking indication that some of the shell-model results for these six active particle nuclei can be discussed in rotational-model terminology. It can also be seen that the shell-model results tend to follow nature when nature deviates from the simple rotational-model scheme. These ideas will be pursued further in the following sections.

TABLE VII. $B(E2, J_i \to J_f)$ for ^{22}Ne $(e^2\,F^4)$.

J_i	J_f	Exp	Present	HMWP	Arima et al.[a]	Rotational[b]
2_1	0_1	$\begin{Bmatrix} 66 \pm 12\ [c] \\ 40 \pm 3\ [d] \end{Bmatrix}$	48	54.9	60.1	47.9
4_1	2_1	54.2 ± 11.7 [e]	66	72.5	65.0	68.4
6_1	4_1		53		66.6	
8_1	6_1		30		44.4	
0_2	2_1		15		6.81	
3_1	2_2		47	83.8	101.0	
5_1	4_2		44		52.2	
2_2	2_1		1.4		6.40	
2_2	0_1		3.7		0.23	
4_2	2_1		0.65		9.58	
4_2	2_2		9.3	25.9	23.3	
4_2	3_1		4.1	56.1	70.2	
5_1	3_1		8.5		41.0	

[a] Reference 5.
[b] Rotational model calculated by HMWP.
[c] Reference 16.
[d] Reference 17.
[e] Reference 15.

FIG. 3. Calculated transition rates for $T = 1 \to T = 1$ transitions in ^{22}Ne.

TABLE VIII. Comparison of calculated and experimental lifetimes (psec) for states in ^{22}Na.

State	Calc	Jones et al.[a]	Kavanagh[b]	Blaugrund et al.[c]	Paul et al.[d]	Pronko et al.[e]	Warburton et al.[f]	Warburton et al.[g]
4_1	16	14.4 ± 0.7	18 ± 7	10.8 ± 1.8	13.4 ± 3	$11.1^{+11.2}_{-3.7}$	>8	
5_1	4.4	5.0 ± 0.7	3.2 ± 1		$\begin{Bmatrix} 3.4 \pm 0.8 \\ 3.14^{+0.62}_{-0.78} \end{Bmatrix}$	$3.9^{+2.2}_{-1.0}$	3.8 ± 0.9	
3_2	2.2				1.87 ± 0.35		$\begin{Bmatrix} 1.6 \pm 0.34 \\ 1.7 \pm 0.6 \end{Bmatrix}$	
3_3	1.8				0.060 ± 0.013		<0.14	
2_1	0.65				0.04 ± 0.01		<0.09	
6_1	0.096							0.052 ± 0.017

[a] Reference 18.
[b] Reference 19.
[c] Reference 20.
[d] Reference 21.
[e] Reference 22.
[f] Reference 23.
[g] Reference 24.

B. Transition Rates

We have calculated the strengths for the $E2$ and $M1$ transitions which connect most of the low-lying levels of ^{22}Na and ^{22}Ne, even though the majority of these are presently not experimentally determined. In addition to the obvious purpose of providing predictions for new experiments to test, we present these calculated strengths so that the various relationships between different model states may be traced and so that alternate techniques for performing microscopic nuclear structure calculations can be checked in detail against an exact shell-model calculation.

Reduced electromagnetic transition rates for various transitions in ^{22}Na and ^{22}Ne are presented in Tables IV and V. Table IV lists both the $B(E2)$ and the $B(M1)$ values for the $T = 0 \to T = 0$ transitions. The $B(M1)$ rates between $T = 0$ states are extremely weak because of Morpurgo's rule. The isovector contribution to the transition vanishes and, since the J part of the isoscalar term cannot

connect two orthogonal states, the effective M^1 operator reduces to a small term $(0.38\bar{s})$. In Table V, the $B(E2)$ values for transitions between $T = 1$ states are presented. Most of the entries deal with ^{22}Ne, while a few ^{22}Na values are presented to indicate the changes which arise when a proton is substituted for a neutron in the $T = 1$ wave functions. The $\Delta T = 1$ transitions in ^{22}Na are predicted to be universally weak, the largest values being ~1.5 e^2 F^4 and the typical values much smaller.

In Fig. 2 all of the $T = 0 \to T = 0$ transitions having calculated $B(E2)$ values greater than 8 e^2 F^4 are displayed. Two nominal rotational bands [by which we mean a group of levels which are connected by strong $E2$ transitions and whose energies

TABLE IX. Comparison of calculated and experimental lifetimes (psec) for states in ^{22}Ne.

State	Calc	Jones et al.[a]	Kutschera et al.[b]
2_1	4.9	4.6 ± 0.5	
4_1	0.32		0.34 ± 0.05
2_1	0.0056		<0.023
6_1	0.064		$0.031^{+0.022}_{-0.014}$

[a] Reference 18.
[b] Reference 25. The lifetime of the 4_1 level represents an average of existing data.

TABLE X. Electric quadrupole and magnetic dipole moments.

State J_n, T	Q_{calc} $(e\,F^2)$	Q_{exp} $(e\,F^2)$	μ_{calc} (μ_N)	μ_{exp} (μ_N)
^{22}Na $1_1, 0$			0.529	0.540 ± 0.009 [a]
$1_2, 0$			0.628	
$3_1, 0$	22	23 ± 2 [b]	1.78	1.746 ± 0.003 [c]
$4_1, 0$	6.8			
$5_1, 0$	-0.90			
$2_1, 1$	-15		1.1	
$2_2, 1$	4.4			
^{22}Ne $2_1, 1$	-14	-18 ± 4 [d]	0.68	
$2_2, 1$	2.3			

[a] This number is a weighted average of the values 0.535 ± 0.010 (Ref. 26) and 0.555 ± 0.017 (Ref. 27).
[b] Q_{exp} obtained from intrinsic quadrupole moment ($+54 \pm 4$) determined by Ref. 14.
[c] Reference 28.
[d] Reference 17.

follow an approximate $J(J+1)$ sequence] are seen, with the 3_1^+ and 1_1^+ states as band heads, as well as a third possible band built upon the 1_2^+ state. Each "band" is relatively well defined, with no large interband transitions. The experimental evidence for the existence of rotational bands in ^{22}Na has been summarized by Garrett et al.[8] In a Nilsson-model interpretation, the level sequence starting with the 3_1^+ state can be identified as a $K = 3$-$T = 0$ band based on the $(\frac{3}{2}^+[211])^2$ Nilsson configuration. The observed levels of this sequence are the 3^+ (ground state), 4^+ (0.89-MeV), 5^+ (1.53-MeV), and 6^+ (3.71-MeV) states. The sequence starting with the 1_1^+ state corresponds to the $K = 0$, $T = 0$ band of the same configuration. The suggested observed members are the 1^+ (0.58-MeV) and 3^+ (1.98-MeV) states. Garrett et al. suggest that a third band based on the $\frac{3}{2}^+[211]$, $\frac{1}{2}^+[211]$ configuration with $K = 1$-$T = 0$ could also exist, with the observed members being 1^+ (1.94

TABLE XI. Spectroscopic factors for single-particle transfer reactions leading to states in ^{22}Na.

| $J_n T$ | E^+ (MeV) | | ^{21}Ne → ^{22}Na | | | | | ^{23}Na → ^{22}Na | | | | |
| | Calc | Exp | 100× $S(j)_{calc}$ | | | 100× $S(l)_{exp}$ [b] | | 100× $S(j)_{calc}$ | | | 100× $S(l)_{exp}$ [c] | |
			$(d_{5/2})$	$(d_{3/2})$	$(s_{1/2})$	$(l=2)$	$(l=0)$	$(d_{5/2})$	$(d_{3/2})$	$(s_{1/2})$	$(l=2)$	$(l=0)$
$0_1 0$	7.54			61								
$1_1 0$	0.22	0.58	76	7	2	65	4	20	2	1	21	<2
$1_2 0$	1.85	1.94	0	22	12	d	<19 [d]	0	3	3		<5 [d]
$1_3 0$	3.79	3.94	30	1	3	33	10	0	0	2	<1	3
$1_4 0$	5.48	4.32	8	7	0	3	<1	0	0	1	<1	<1
$2_1 0$	2.60	3.06	4	30	9	56	12	0	3	0	3	<1
$2_2 0$	3.23	4.36 [a]	2	13	20	<10	66	1	2	4	2	2
$2_3 0$	4.93		9	2	10			6	0	3		
$2_4 0$	5.33		9	11	12			1	0	0		
$3_1 0$	0.00	0.00	44	3		47		56	3		51	
$3_2 0$	1.59	1.98	42	0		27		36	1		25	
$3_3 0$	2.88	2.97	9	4		32		12	1		<2	
$3_4 0$	4.16		1	21				3	2			
$4_1 0$	0.86	0.89	101			80		58			49	
$4_2 0$	4.34		1					0				
$4_3 0$	5.00							0				
$4_4 0$	5.80							1				
$0_1 1$	0.66	0.66		9		<40			2		<18	
$0_2 1$	6.64	6.83		5					0		<1	
$0_3 1$	7.68			1					0			
$1_1 1$	5.69		59	2	10			1		2		
$1_2 1$	7.14		0	1	48			1		4		
$1_3 1$	8.91		0	5	2			3	1	3		
$1_4 1$	9.48		0	33	7			0	3	0		
$2_1 1$	2.05	1.95	94	1	0	<100 [d]	<12 [d]	144	3	21	<147 [d]	<15 [d]
$2_2 1$	4.80	5.16	12	11	10	28	12	23	3	0	39	18
$2_3 1$	5.46		0	5	21			8	2	4		
$2_4 1$	6.71		0	0	2			6				
$3_1 1$	6.07		3	18				13	2	15		
$3_2 1$	6.97		13	0				26	0	26		
$3_3 1$	8.06		1	9				15	0	15		
$3_4 1$	8.80		1	0				14	0	14		
$4_1 1$	4.15	4.07	3			4		42			42	44
$4_2 1$	6.15		25					5			5	
$4_3 1$	7.09		16									
$4_4 1$	7.50		4									

[a] The spin assignment for the 4.36-MeV state is tentative.

[b] ^{21}Ne(^{3}He, d) experimental spectroscopic factors are from Ref. 8.

[c] ^{23}Na(^{3}He, α) experimental spectroscopic factors are from Ref. 9.

[d] States at 1.94 and 1.95 MeV were unresolved.

MeV) and 2^+ (3.06 MeV). The choice of whether the 3^+ member of this band should be the 2.97-MeV or the 4.77-MeV 3^+ state is unclear. The calculations shown in Fig. 2 indicate that the model state 3_3^+ at 2.88 MeV [and hence the 3^+ (2.97-MeV) empirical level] belongs in this group.

In Table VI the $B(E2)$ values for the $T = 0 \rightarrow T = 0$ transitions in ^{22}Na are compared with existing experimental values[14, 15] and with the calculations of HMWP and of Arima et al.[5] The rotational values are taken from HMWP. It is seen that there is good agreement between the experimental values and the present calculations and the rotational- and shell-model calculations of HMWP. In contrast, the calculations of Arima et al. are in complete disagreement with all other results, a discrepancy previously noted by those authors.

Transitions in ^{22}Ne having calculated $B(E2)$'s greater than 8 e^2 F^4 are shown in Fig. 3. Three possible bands exist, with no large interband transitions. The $K = 0$ ground-state band is well established experimentally, with observed levels as 0^+ (ground state), 2^+ (1.28-MeV), 4^+ (3.36-MeV), 6^+ (6.35-MeV), and the 8^+ (11.01-MeV) states. The apparent $K = 2$ band built on the 2_2^+ state was noted by HMWP, with the possible experimental partners for the 2_2^+, 3_1^+, and 4_3^+ levels as the 2^+ (4.46-MeV), 3^+ (5.63-MeV), and the $2 \leqslant J \leqslant 6$ (6.68-MeV) states. The band beginning with the 4_2^+ state has not been previously suggested. This 4_2^+ state was taken by HMWP as the 4^+ state in the "$K = 2$" band. The 0_2^+ state at 5.98 MeV can be identified with the empirical 0^+ level at 6.24 MeV. It has the interesting property of sizable calculated transition probabilities to both the "$K = 2$"

and the "$K = 0$" bands.

In Table VII $B(E2)$ values in ^{22}Ne from the present calculation are compared with experimental values[15-17] and with those calculated by HMWP (shell-model and rotational) and by Arima et al.[5] For the $K = 0$ ground-state band, there is good agreement between all of the calculations and experiment, allowing for the discrepancy in the experimental values for the $2_1^+ \rightarrow 0_1^+$ transition. However, the transition rates calculated by Arima et al. for the $6_1^+ \rightarrow 4_1^+$ and $8_1^+ \rightarrow 6_1^+$ transitions are somewhat larger than in the present calculation. The transitions $4_2^+ \rightarrow 2_2^+$, $4_2^+ \rightarrow 3_1^+$, and $3_1^+ \rightarrow 2_2^+$ were taken by HMWP as transitions within the $K = 2$ band because of the values shown in Table VII. Since the $4_2^+ \rightarrow 3_1^+$ transition has such a relatively low value in the present calculation and yet the 4_2^+ state is strongly connected to higher states, as was seen in Fig. 3, it is concluded that this state does not belong in our "$K = 2$" band. A few other transitions are compared with values calculated by Arima et al. There is no obvious correlation in the values.

The only $B(M1)$ values calculated for ^{22}Ne are for the J_i^{π}, $T = 1 \rightarrow J_f^{\pi}$, $T = 1$ transitions $2_2 \rightarrow 2_1$ (0.30μ_N^2), $2_3 \rightarrow 2_1$ (0.014μ_N^2), and $2_4 \rightarrow 2_1$ (0.197 μ_N^2), where μ_N is the nuclear magneton.

The values of $B(E2)$ for the two lowest transitions in the ground-state band of ^{22}Mg($T_z = +1$) have also been calculated. For the $2_1^+ \rightarrow 0_1^+$ transition, the present calculation gives a value of 64 e^2 F^4, smaller than the experimental value of 104^{+44}_{-24} e^2 F^4 (quoted in Ref. 5) and comparable to the value of 74.5 e^2 F^4 calculated by Arima et al.[5] For the $4_1^+ \rightarrow 2_1^+$ transition, the present value of 77 e^2 F^4 is also close to the value of 83.1 e^2 F^4 calculated by Arima et al.

SPECTROSCOPIC FACTORS FOR ^{21}Ne $\rightarrow$ ^{22}Na
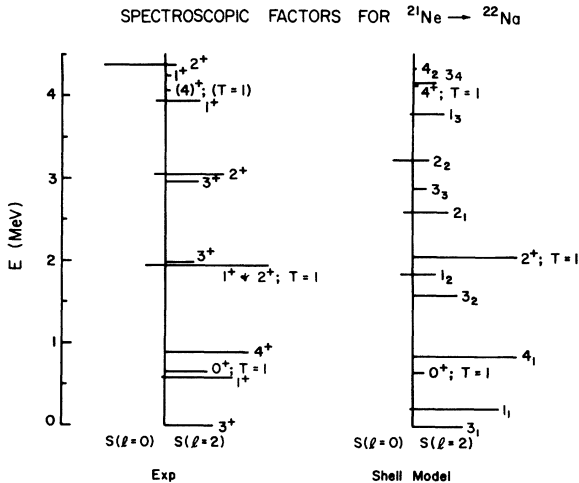
FIG. 4. Spectroscopic factors for the ^{21}Ne(^{3}He,d)^{22}Na reaction. The length of the line is directly proportional to the magnitude of the spectroscopic factor.

SPECTROSCOPIC FACTORS FOR ^{23}Na $\rightarrow$ ^{22}Na
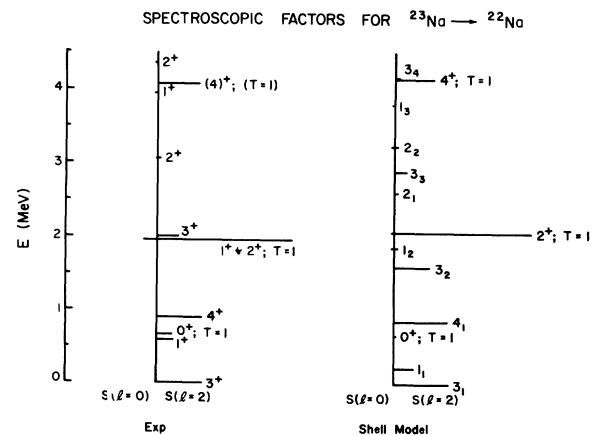
FIG. 5. Spectroscopic factors for the ^{23}Na(^{3}He,α)^{22}Na reaction. The length of the line is directly proportional to the magnitude of the spectroscopic factor.

C. Lifetimes and Moments

From the transition rates presented in the previous section it is possible to calculate partial and total decay widths for the various levels and thus determine their lifetimes. In Table VIII the calculated mean lifetimes for ^{22}Na levels are compared with existing data.[18-24] A similar comparison[18, 25] for some states in ^{22}Ne is presented in Table IX.

Electric quadrupole (static) and magnetic dipole moments are shown in Table X along with some measured[17, 26-28] values. The calculated value of Q for the ^{22}Na ground state is in good agreement with the measured value, whereas the calculated value for the 2_1^+ state in ^{22}Ne has the correct sign but is significantly smaller in magnitude than the observed value. Similar calculations by Arima et al.[5] for ^{22}Ne gave a value $(-15.4\ e\ F^2)$ only slightly larger than the present value, whereas for the ground state of ^{22}Na they obtained the value $-9.36\ e\ F^2$. For the ^{22}Na ground state, calculations by HMWP gave values of $22.1\ e\ F^2$ for the $K + {}^{17}$O interaction and $21.6\ e\ F^2$ for an adiabatic rotational model. These values compare with the present value for ^{22}Na of $22\ e\ F^2$.

The magnetic moments shown in Table X for the 1_1 and 3_1 states of ^{22}Na are also in close agreement with experimental values. The present value for the 3_1^+ state $(1.78\mu_N)$ is similar to those of HMWP $(1.82\mu_N)$ and of Arima et al. $(1.83\mu_N)$. However, for the 1_1^+ state, the present value of $0.529\mu_N$ is in better agreement with experiment than the value of $0.787\mu_N$ obtained by Arima et al.

D. Spectroscopic Factors

Single-particle spectroscopic factors are presented in Table XI for the transfer reactions which connect ^{21}Ne and ^{23}Na with the $T = 0$ and $T = 1$ levels of $A = 22$. The distributions of $l = 0$ and $l = 2$ strengths are shown in Figs. 4 and 5, with the lengths of the lines being directly proportional to the spectroscopic strengths. The experimental values are from the $(^3$He, $d)$ reaction[8] and the $(^3$He, $\alpha)$ reaction.[9] Since the ground-state spins of both ^{21}Ne and ^{23}Na are $\frac{3}{2}^+$, states with $J = 0, 3, 4$ can be populated only by $l = 2$ transfer, whereas the 1^+ and 2^+ states can be populated by both $l = 0$ and $l = 2$ transfers. The ^{21}Ne and ^{23}Na wave functions are calculated with the same Hamiltonian that we use for $A = 22$. The model basis space for the $A = 23$ calculation was truncated as described in Ref. 4.

The results for ^{21}Ne$(^3$He, $d)^{22}$Na are shown in Fig. 4. The ground-state $l = 2$ strength is well accounted for. The only other accessible member of the ground-state band, i.e., the $4^+(4_1)$, also shows agreement. The $1^+(1_1)$ and $3^+(3_2)$ members of the $K = 0$ band show agreement in relative $l = 2$ strength, with the calculated strengths being about 30% too large.

The strengths of the 0^+, 2^+, and 4^+ $T = 1$ states also appear to be fairly well accounted for, with the 0^+ strength predicted to be lower than the experimental upper limit shown. Because the 1.94 (1^+) and 1.95 $(2^+,\ T = 1)$ states were experimentally unresolved, only a qualitative agreement between the 2^+, $T = 1$ states can be proposed. Ex-

TABLE XII. Spectroscopic factors for ^{21}Ne $\rightarrow {}^{22}$Ne.

J_n	E^* Calc	E^* Exp [a]	$100 \times S(j)_{calc}$ $(d_{5/2})$	$(d_{3/2})$	$\Sigma(l=2)$	$(s_{1/2})$	$(l=2)$ [b]	$100 \times S(l)_{exp}$ $(l=0)$ [b]	$(l=2)$ [c]	$(l=0)$ [c]
0_1	0	0		9	9		≤ 22			
1_1	5.03	(5.36)	59	2	61	10	d	d	e	e
2_1	1.39	1.28	94	1	95	0	140	≤ 3	135	
2_2	4.14	4.46	12	11	23	10	24	6	34	11
2_3	4.80	(5.33)		5	5	21	d	d	e	e
3_1	5.41	(5.64)	3	18	21		12		24	
4_1	3.49	3.36	3		3		≤ 6			
4_2	5.49	5.52	25		25		33		56	

[a] Spin assignment is tentative for states in parentheses.

[b] $E_d = 10.2$ MeV (Ref. 29).

[c] $E_d = 3.22$ MeV (Ref. 30).

[d] States at 5.33 and 5.36 MeV unresolved. $\Sigma(2J_f + 1)\ S_{exp}(l = 2) \leq 2.5$ and $\Sigma(2J_f + 1)\ S_{exp}(l = 0) = 2.2$ compared with $\Sigma(2J_f + 1)\ S_{th}(l = 2) = 2.08$ and $\Sigma(2J_f + 1)\ S_{th}(l = 0) = 1.35$.

[e] States at 5.33 and 5.36 MeV unresolved. $(2J_f + 1)\ S_{exp}(l = 2) = 2.76$ and $\Sigma(2J_f + 1)S_{exp}(l = 0) = 2.03$ compared with $(2J_f + 1)\ S_{th}(l = 2) = 2.08$ and $\Sigma(2J_f + 1)\ S_{th}(l = 0) = 1.35$.

periment and calculation both say that the strength to the 4_1^+, $T = 1$ state is weak.

Transitions to members of the $K = 1$ band built on the $1^+(1_2)$ state also are in qualitative agreement with the calculations. The unresolved 1.94 (1^+) and 1.95 $(2^+$, $T = 1)$ states show an upper limit $l = 0$ strength comparable to the calculated strength for the 1_2 state. The 2_1 and 3_3 states show similar agreement with the 3.06 (2^+) and 2.97 (3^+) states, for both the $l = 0$ and $l = 2$ strengths.

Two other states in Fig. 4 show agreement between calculation and experiment. The 3.94 (1^+) state agrees very well with the $l = 2$ strength predicted for the 1_3 state but has three times as much (0.10 vs 0.03) $l = 0$ strength. The 4.36 (2^+) state can be identified with the 2_2^+ state, although there is no quantitative agreement. Comparing the $l = 0$ and $l = 2$ strengths calculated for the other 2^+ states, the 2_2 state is the only one that has more $l = 0$ than $l = 2$ strength, which is the characteristic of the 4.36 (2^+) state.

There is also quantitative agreement for another state which is presented in Table XI but not shown in Fig. 4. The 5.16 $(2^+$, $T = 1)$ state has experimental strengths of 0.12 $(l = 0)$ and 0.28 $(l = 2)$ as compared with the calculated strengths 0.10 $(l = 0)$ and 0.23 $(l = 2)$.

The results for the neutron-pickup reaction ^{23}Na(^{3}He, ^{4}He)^{22}Na are displayed in Fig. 5. As before, transitions to the ground-state band show quantitative agreement between experiment and calculation. The observed relative strengths of the "$K = 0$" band also agree with the calculations, but the calculations predict larger over-all values, as was the case in the stripping reaction. The observed strengths for $T = 1$ levels appear to agree rather well with the model results, except possibly in the case of the 0^+ state, although for this state the experimental value displayed is an upper limit. For the higher-lying states, the observed strengths are very small, again in qualitative agreement with the predictions.

In Table XII, calculated spectroscopic factors are compared with experimental values[29, 30] for the ^{21}Ne(d, p)^{22}Ne reaction. There is generally good agreement between the calculated and experimental values except for the 3_1 state seen

for $E_d = 10.2$ MeV and the 4_2 state seen for $E_d = 3.22$ MeV.

IV. SUMMARY

The shell-model calculations presented in this paper for $A = 22$ were made in the full basis of Pauli-allowed states for six nucleons distributed among the $0d_{5/2}$-$1s_{1/2}$-$0d_{3/2}$ orbits. The calculations used an empirically modified version of Kuo's two-body Hamiltonian that was adjusted to give a best fit to 72 energy levels in this mass region, and the single-particle energy spectrum observed in ^{17}O. A large number of observables were calculated with this Hamiltonian, and the predictions compared with other pertinent calculations and with experiments, wherever possible. These observables included excitation energies, electromagnetic transition rates and lifetimes of levels, electric and magnetic moments, and spectroscopic factors for single-nucleon transfer reactions. With only a few exceptions, the calculated quantities are in agreement with existing experimental data. These calculations thus provide a comprehensive theoretical framework for understanding observed phenomena of the $A = 22$ systems, and this framework is rigorously connected to equally successful theoretical explanations of the lighter sd-shell nuclei. The various "rotational" aspects of the $A = 22$ nuclei which are manifest in the experimental data are found to be calculable consequences of coherent motion among the nucleons distributed over the full sd-shell space. Moreover, the present calculations predict that these "rotational" phenomena extend through many presently unexplored levels. Finally, comparisons of the present results with those of previous calculations demonstrate the effects both of modifying the two-body Hamiltonian and of truncating the active model space.

V. ACKNOWLEDGMENTS

[1]J. B. French, E. C. Halbert, J. B. McGrory, and S. S. M. Wong, in *Advances in Nuclear Physics*, edited by M. Baranger and E. Vogt (Plenum, New York, 1969), Vol. 3.

[2]E. C. Halbert, J. B. McGrory, B. H. Wildenthal, and S. P. Pandya, in *Advances in Nuclear Physics*, Ref. 1, Vol. 4.

[3]Y. Akiyama, A. Arima, and R. Sebe, Nucl. Phys. A138, 273 (1969).

[4]J. B. McGrory and B. H. Wildenthal, Phys. Letters 34B, 373 (1971).

[5]A. Arima, M. Sakakura, and T. Sebe, Nucl. Phys.

A170, 273 (1971).

[6]B. H. Wildenthal, to be published.

[7]T. T. S. Kuo, Nucl. Phys. A103, 71 (1967).

[8]J. D. Garrett, R. Middleton, and H. T. Fortune, Phys. Rev. C 4, 165 (1971).

[9]J. D. Garrett, H. T. Fortune, and R. Middleton, Phys. Rev. C 4, 1138 (1971).

[10]I. Kelson, Phys. Rev. 134, B267 (1964).

[11]R. W. Ollerhead, G. F. R. Allen, A. M. Baxter, B. W. J. Gillespie, and J. A. Kuehner, Can. J. Phys. 49, 594 (1971); P. Neogy, Ph.D. thesis, University of Pennsylvania, 1971 (unpublished).

[12]W. Scholz, P. Neogy, K. Bethge, and R. Middleton, Phys. Rev. Letters 22, 949 (1969).

[13]C. Broude, W. G. Davies, and J. S. Forster, Phys. Rev. Letters 25, 944 (1970).

[14]E. K. Warburton, A. R. Poletti, and J. W. Olness, Phys. Rev. 168, 1232 (1968).

[15]S. J. Skorka, J. Hertel, and T. W. Retz-Schmidt, Nucl. Data 2, 347 (1966).

[16]K. Nakai, F. S. Stephens, and R. M. Diamond, Nucl. Phys. A150, 114 (1970).

[17]D. Schwalm and B. Povh, Phys. Letters 29B, 103 (1969); and private communication.

[18]K. W. Jones, A. Z. Schwarzchild, E. K. Warburton, and D. B. Fossan, Phys. Rev. 178, 1773 (1969).

[19]R. W. Kavanagh, Bull. Am. Phys. Soc. 12, 913 (1967).

[20]A. E. Blaugrund, A. Fisher, and A. Schwarzchild, Nucl. Phys. A107, 411 (1968).

[21]P. Paul, J. W. Olness, and E. K. Warburton, Phys. Rev. 173, 1063 (1968).

[22]J. G. Pronko, C. Rolfs, and H. J. Maier, Phys. Rev. 167, 1066 (1968).

[23]E. K. Warburton, J. W. Olness, and A. R. Poletti, Phys. Rev. 160, 938 (1967).

[24]E. K. Warburton, L. E. Carlson, G. T. Garvey, D. A. Hutcheon, and K. P. Jackson, Nucl. Phys. A136, 160 (1969).

[25]W. Kutschera, D. Pelte, and G. Schrieder, Nucl. Phys. A111, 529 (1968).

[26]A. W. Sunyar and P. Thieberger, Phys. Rev. 151, 910 (1966).

[27]H. Schmidt, J. Morgenstern, H. J. Körner, J. Braunsfurth, and S. J. Skorka, Phys. Letters 24B, 457 (1967).

[28]L. Davis, Jr., D. E. Nagle, and J. R. Zacharias, Phys. Rev. 76, 1068 (1949).

[29]A. J. Howard, J. G. Pronko, and R. G. Hirko, Nucl. Phys. A150, 609 (1970).

[30]B. Chambon, D. Drain, M. Yaker, G. Dumazet, G. Salmer, H. Beaumevieille, M. Lambert, and Nguyen Van Sen, Nucl. Phys. A136, 311 (1969).

Accurate Excitation Energies of ^{27}Al from 5.4 to 8.4 MeV and Identification of $T = \frac{3}{2}$ Levels*

E. A. Kamykowski and C. P. Browne

Department of Physics, University of Notre Dame, Notre Dame, Indiana 46556

(Received 8 May 1972)

Excitation energies of 57 states in ^{27}Al from 5.4 to 8.4 MeV were measured with accuracy of ±2 to ±3 keV. Energies of particles from the ^{27}Al$(p, p')^{27}$Al and ^{29}Si$(d, \alpha)^{27}$Al reactions were measured with the Notre Dame 50-cm broad-range spectrograph. In the range 5.4 to 7.0 MeV values agree within 5.5 keV with other recent (p, p') work and within 4.6 keV with recent γ-ray work. Systematic discrepancies in the (p, p') values increasing to 20 keV at 8.3 MeV are found. Resolution was sufficient to measure excitation energies separated by 5 keV. The existence of two pairs of closely spaced levels in the region of the first $T = \frac{3}{2}$ state was confirmed. The first and second $T = \frac{3}{2}$ levels were identified by the low cross section of the ^{29}Si$(d, \alpha)^{27}$Al reaction. The value of this accurately measured proton spectrum for calibration purposes is discussed.

I. INTRODUCTION

This work was inspired by comments of Barnes,[1] that the strong excitation by the ^{29}Si$(d, \alpha)^{27}$Al reaction of a level[2] at the position of the first $T = \frac{3}{2}$ state in ^{27}Al, probably did not represent a strong violation of the isobaric-spin-selection rule but rather the existence of a $T = \frac{1}{2}$ level very near the $T = \frac{3}{2}$ level. We soon found disagreements between our excitation energies and those recently measured elsewhere and this led us to extend the work

to provide a very accurate set of excitation energies up to 8.4 MeV. An accurately known spectrum such as this, containing many sharply defined groups, should be very useful for energy calibration of spectrographs and other detectors. This range of excitation energies, which includes the second $T = \frac{3}{2}$ state, was measured with both the ^{29}Si$(d, \alpha)^{27}$Al and ^{27}Al$(p, p')^{27}$Al reactions.

A number of precision measurements of excitation energies of the ^{27}Al nucleus have been made through the years. Browne[2] used the ^{29}Si$(d, \alpha)^{27}$Al